

A model relating Eulerian spatial and temporal velocity correlations

By MURALI R. CHOLEMARI
AND JAYWANT H. ARAKERI

Department of Mechanical Engineering, Indian Institute of Science, Bangalore, 560012, India

(Received 24 September 2004 and in revised form 18 August 2005)

In this paper we propose a model to relate Eulerian spatial and temporal velocity autocorrelations in homogeneous, isotropic and stationary turbulence. We model the decorrelation as the eddies of various scales becoming decorrelated. This enables us to connect the spatial and temporal separations required for a certain decorrelation through the ‘eddy scale’. Given either the spatial or the temporal velocity correlation, we obtain the ‘eddy scale’ and the rate at which the decorrelation proceeds. This leads to a spatial separation from the temporal correlation and a temporal separation from the spatial correlation, at any given value of the correlation relating the two correlations. We test the model using experimental data from a stationary axisymmetric turbulent flow with homogeneity along the axis.

1. Introduction

In turbulent flows, usually two types of correlations are used: Lagrangian, where a correlation is calculated following a fluid particle, and Eulerian, where the correlations are in general with spatial and temporal separations. Thus there could be Eulerian spatial, Eulerian temporal and Eulerian spatio-temporal correlations. Till recently, correlation measurements were mostly made using probes at two spatial points. Favre and co workers (Favre 1965; Favre, Gaviglio & Dumas 1957, 1958), report extensive space–time correlations using hot wires at two locations. In the case of time-periodic flows, spatial structures were inferred using phase averaging (Zaman & Hussain 1981; LeBoeuf & Mehta 1995). Now, with particle image velocimetry (PIV) and direct numerical simulation (DNS) it is possible to get spatial correlations involving many spatial points.

DNS of isotropic turbulence has been extensively used to obtain the Lagrangian statistics (see for e.g. Riley & Patterson 1974; Yeung & Pope 1989; Squires & Eaton 1989; Yeung 2001). A survey of the Lagrangian studies of turbulence with an emphasis on DNS is in Yeung (2002). Fewer Eulerian statistics are reported in the context of isotropic turbulence.

In the absence of spatial data, spatial statistics have been widely inferred from single-point temporal measurements using the ‘frozen’ turbulence hypothesis of Taylor (1938). The hypothesis assumes that the timescales of the turbulence are large compared to the advection time in the spatial extent considered; then $\psi(\mathbf{x}, \tau) = \psi(\mathbf{x} - U\tau, 0)$ for some quantity ψ ; U is the advection velocity. Possible causes for errors when applying the hypothesis are: temporal evolution of the flow field, spatial non-uniformity of the convection velocity, anisotropy produced by shear, and aliasing due to unsteadiness of the convection velocity. These errors and their

corrections are described in Lin (1953), Lumley (1965), Heskestad (1965) and Gledzer (1997). Corrections to the velocity spectra due to the hypothesis are also detailed in Fisher & Davies (1964) and Wyngaard & Clifford (1977). The hypothesis is found to be valid in general for velocity statistics as well as temperature statistics away from the walls and at low turbulence intensities (Antonia, Phan-Thien & Chambers 1980; Browne, Antonia & Rajagopalan 1983; Piomelli, Balint & Wallace 1989). The application of the hypothesis in the case of interacting coherent structures yields poor results (Zaman & Hussain 1981; LeBoeuf & Mehta 1995). The results are also poor in the case of three dimensional scalar structures (Dahm & Southerland 1997). A mean flow is present in all these studies.

The extension of the Taylor hypothesis to flows without a mean flow is called the random Taylor hypothesis which is concerned with the sweeping of the turbulence field past a fixed observer by the larger eddies (Tennekes 1975; Yeung & Pope 1989; Chen & Kraichnan 1989; Brouwers 2004; Yeung & Sawford 2002). It is required that the large and small scales of turbulence are separated and that local and the convective accelerations of turbulence be anti-aligned, leading to negligible Lagrangian acceleration, and hence causing the advection of a ‘frozen’ field (Tennekes 1975; Tsinober, Vedula & Yeung 2001; Brouwers 2004). Use has been made of this hypothesis to relate Eulerian spatial and temporal spectra (Tennekes 1975; Nelkin & Tabor 1990) and to explain the spectral broadening of Eulerian time spectra at high frequencies. Pinsky, Khain & Tsinober (2000) study the various contributions to the acceleration and show that the use of the hypothesis is questionable for low values of the Reynolds numbers. Using the random Taylor hypothesis, Brouwers (2004) gives a theoretical expression to relate Eulerian spatial and temporal structure functions. The relation is valid for small times.

In this paper we propose a model to relate spatial and temporal Eulerian two-point correlations in stationary, isotropic and homogeneous turbulence. The model is applicable in the absence of mean flow but includes the effects of sweeping by the large eddies. It would modify the application of the Taylor hypothesis in the case of turbulence with mean flow. We test the model using measurements in a quasi-steady turbulent flow with zero mean, driven purely by buoyancy and which is homogeneous in one direction (Cholehari 2004).

2. Model

The model is concerned with the relation between Eulerian two-point spatial and Eulerian temporal velocity correlations in homogeneous, isotropic and stationary turbulence, with zero mean velocity ($\langle u_i \rangle = 0$). In such a flow the same processes produce both spatial and temporal correlations. We look at these processes as resulting in eddies with similar spatial and temporal distributions. These eddies have a range of scales, from the largest to the viscous or Kolmogorov length scale. The larger eddies occur less often compared to the smaller eddies. Also, as can be seen from the velocity spectrum, the velocities of the various eddy scales are different. The velocity correlation functions are the result of all this information: the eddy scale, the velocity at that scale and the frequency of occurrence of the eddies at that scale. Although simplistic, this perspective serves as a starting point for establishing a model for relating spatial and temporal correlations.

Consider the *Eulerian two-point spatial autocorrelation*

$$\mathcal{C}_{u_i u_i}^S(r_j, t) = \frac{\langle u_i(\mathbf{x}, t) u_i(\mathbf{x} + r_j, t) \rangle}{u_i' u_i'}$$

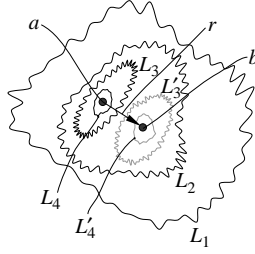


FIGURE 1. Schematic of eddy decorrelation. The decorrelation with spatial separation r can be associated with an eddy scale. Only eddies of size larger than r contribute to the correlation.

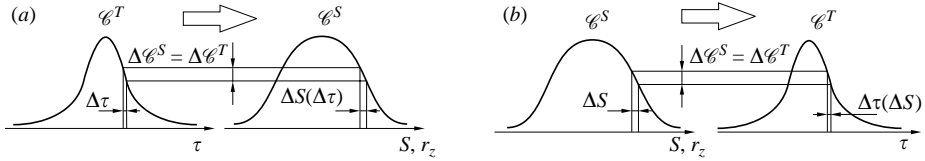


FIGURE 2. Schematic of the model: (a) temporal to spatial and (b) spatial to temporal.

where u_i is a velocity component, u'_i is its RMS value, and r_j is the separation in the j -direction. The correlation function is equal to 1 for $r_j = 0$ and reduces in value with increasing r_j . The decorrelation with spatial separation can be associated with an eddy scale. At small separations, the velocity correlation will have a contribution from the larger eddies, but not from the smaller ($\ell < r_j$) eddies; here ℓ refers to the eddy scale. With increasing separation more and more eddies stop contributing to the correlation. Another way to look at this would be as the decorrelation between the smallest eddies (corresponding to the origin of the correlation) and the progressively larger eddies (corresponding to the increasing separation), in which the smaller eddies are embedded. This is illustrated in figure 1 where four eddy sizes L_1 to L_4 are shown, L_1 being the largest; let their sizes be r_{L1} , r_{L2} etc. Consider a separation $r > r_{L3}$, r_{L4} but $r < r_{L2}$, r_{L1} . Consider the reference point at a . Eddies L_1 , L_2 , L_3 and L_4 contribute to the correlation, while L'_3 and L'_4 , being smaller than r , do not.

The *Eulerian temporal autocorrelation*,

$$\mathcal{C}_{u_i u_i}^T(\tau) = \frac{\langle u_i(\mathbf{x}, t) u_i(\mathbf{x}, t + \tau) \rangle}{u'_i u'_i}$$

similarly starts with value 1 at zero temporal separation (τ) and reduces with increasing τ . As τ increases, progressively larger eddies are swept away from the reference point, causing the decorrelation. We can relate the decorrelation with separation time to the decorrelation between the smallest eddies at initial times to larger eddies at later times. This relates the eddy scale to the temporal separation τ and decorrelation. The implicit assumption in the model is that each eddy makes a certain contribution, which is constant within the eddy, to the correlation and this loosely defines the eddy in the sense of the velocity correlation functions.

Our aim in this paper is to propose a model that will give $\mathcal{C}_{u_i u_i}^S(r_i)$ given $\mathcal{C}_{u_i u_i}^T(\tau)$, and give $\mathcal{C}_{u_i u_i}^T(\tau)$ given $\mathcal{C}_{u_i u_i}^S(r_i)$, i.e. relate the longitudinal spatial correlations to the temporal correlation and vice versa. We obtain the spatial separation S for a temporal separation τ such that $\mathcal{C}_{u_i u_i}^S(S) = \mathcal{C}_{u_i u_i}^T(\tau)$ and vice versa (figure 2).

We need to track the decorrelation to relate the eddy scale (and the spatial separation) to the temporal separation. As mentioned earlier, with increasing time of separation τ , progressively larger eddies, of scale $\ell(\tau)$, stop contributing to the correlation. To see how $\ell(\tau)$ changes with τ , we note that, at τ , some of the motions at scales $\ell(\tau)$ and larger contribute to the correlation while none of the smaller scales contribute. In addition, these motions which are correlated result in the temporal and spatial correlations $u'^2 \mathcal{C}_{uu}^T(\tau)$ and $u'^2 \mathcal{C}_{uu}^S(\ell(\tau))$. Since motions at $\ell(\tau)$ and beyond are correlated while those below $\ell(\tau)$ are uncorrelated and the scale $\ell(\tau)$ has an effective velocity $u' \sqrt{\mathcal{C}_{uu}^S(\ell(\tau))} = u' \sqrt{\mathcal{C}_{uu}^T(\tau)}$, decorrelation proceeds at $u' \sqrt{\mathcal{C}_{uu}^S(\ell(\tau))} = u' \sqrt{\mathcal{C}_{uu}^T(\tau)}$.

Additional information can be obtained by reasoning slightly differently. We consider the motion of a hypothetical particle under the action of only the correlated part of the eddies. At the smallest eddy scale, the sweeping action of the larger eddies plus the inherent velocity at the smallest eddies together contribute to the motion. Looking at the spatial correlation function, the effective velocity of the correlated motions, with which the hypothetical displacement takes place, is $u' \sqrt{\mathcal{C}_{uu}^S(r=0)} = u'$. Also, these displacements are related to the longitudinal correlation function and not the transverse correlation function. One can visualize this by choosing an origin and a direction at random and seeing that the longitudinal displacements along that direction – more likely away from the origin as the correlation function is decreasing away from the origin – add up, and transverse displacements, which are equally likely in all the directions in the plane normal to the chosen direction, cancel out. And as the choice of the direction is arbitrary, the progress of the decorrelation is spherical, as expected because of isotropy.

At a later time, when the hypothetical particle is at a distance ℓ away from the initial location, it is under the action of eddies of size $> \ell$. The corresponding spatial separation is ℓ and the correlation would have dropped down to $\mathcal{C}_{uu}^S(\ell)$. The velocity arising out of the correlated part of the eddies with which the hypothetical displacement takes place is $u' \sqrt{\mathcal{C}_{uu}^S(\ell)}$. Thus, using the decorrelation information from the spatial longitudinal correlation function, one obtains a ‘sampled’ velocity field, $u' \sqrt{\mathcal{C}_{uu}^S(\ell)}$. The time that is an integrated effect of this velocity and the eddy scale corresponds to the separation time in the temporal correlation where the eddy decorrelation is associated with the separation time through the eddy scale. And thus we relate the spatial and temporal correlations.

The inverse of this process would be to obtain the spatial correlation function from the temporal correlation function. To obtain the spatial scale of the eddies, we use the decorrelation information from the temporal correlation function to obtain a sampled velocity field, $u' \sqrt{\mathcal{C}_{uu}^T(\tau)}$. This velocity field, along with the associated time of decorrelation, is used to obtain the lengthscale of decorrelation, and thus the spatial separation.

Since the eddy scale information in temporal correlation comes from the longitudinal correlation function, when we consider the correspondence of the temporal correlation and transverse spatial correlation, the factors that contribute to the correlation – the eddy scale, velocity at the eddy scale, frequency of occurrence of the eddies – cannot be linked consistently. Thus the extension of these arguments to the transverse correlations would yield poorer results compared to the longitudinal case.

In addition, not all the motions of an eddy contribute to the correlations; for example, rigid body rotation does not contribute to the longitudinal correlation. However, this is equally true for the spatial and temporal correlations. These are the

uncorrelated motions and would not be used in the model to construct the sampled velocity field.

In non-isotropic turbulence, the spatial decorrelation would be different in different directions and hence the contributions of the transverse velocities to decorrelation would need to be accounted for. The present model cannot do this. Inhomogeneity would bring about this situation as well, causing anisotropy. If the flow is not stationary, the way in which the decorrelation is related to the eddy size and temporal separation would change with time of separation, causing inhomogeneity in space. However in stationary axisymmetric flows with homogeneity in the axial direction, when we consider the longitudinal correlation along the axis, the arguments leading to the model (transverse contributions to eddy-decorrelation cancel out, longitudinal correlation determines eddy-decorrelation) are seen to be valid. In the experiments considered to test the model we have such a case and the model performs well.

We next describe the implementation of the physical arguments detailed above.

2.1. Spatial from temporal

Consider the two-point spatial velocity correlation $\mathcal{C}_{u_i u_i}^S(r_i)$ and the temporal correlation $\mathcal{C}_{u_i u_i}^T(\tau)$. We would like to relate the two as

$$\mathcal{C}_{u_i u_i}^S(\mathcal{S}_i(\tau)) = \mathcal{C}_{u_i u_i}^T(\tau); \quad (2.1)$$

where the *correlated displacement* $\mathcal{S}_i(\tau)$ is the spatial separation r_i of the spatial correlation function $\mathcal{C}_{u_i u_i}^S(r_i)$, such that the correlation equals the temporal correlation at that time, $\mathcal{C}_{u_i u_i}^T(\tau)$. The velocity u_d^T effects the displacement $\mathcal{S}_i(\tau)$.

$$\mathcal{S}_i(\tau) = \int_0^\tau u_d^T(t) dt. \quad (2.2)$$

Further implementation requires the modelling of u_d^T .

Consider $\mathcal{C}_{ww}^T(\tau)$ for example. We propose the following model for the velocity u_d^T :

$$(u_d^T(\tau))^2 = u_s^2 \mathcal{C}_{u_i u_i}^T(\tau) = w'^2 \mathcal{C}_{ww}^T(\tau), \quad (2.3)$$

where u_s^2 is a scaling velocity that depends on the correlation considered. We take $u_s = w'$ for $\mathcal{C}_{ww}^T(\tau)$. The simplest model would have been to take $u_d^T = w'$, but in that case the effect of the decorrelation of the smaller eddies with increasing τ is not modelled. This attenuation is given by $\mathcal{C}_{ww}^T(\tau)$. The sampled velocity $w'^2 \mathcal{C}_{ww}^T(\tau)$ is homogeneous, but depends on τ . The displacement $\mathcal{S}_z(\tau)$ brings the spatial dependence associated with timescale τ into the homogeneous temporal correlation. $\mathcal{S}_z(\tau)$ and the corresponding decorrelation give the spatial correlation $\mathcal{C}_{ww}^S(r_z)$. Equations (2.1), (2.2) and (2.3) together constitute the model. This process is schematically shown in figure 2(a).

We note that in the case of temporal velocity correlations, there is only one set of directions, those corresponding to the velocities. Thus one cannot obtain transverse spatial correlations from the temporal correlations, which require two sets of directions. One can obtain only the longitudinal spatial velocity correlations from temporal velocity correlations.

Further, on differentiating (2.1) with τ and using the chain rule, we obtain

$$\frac{\Delta \mathcal{S}}{\Delta \tau} \simeq \frac{d\mathcal{S}_i(\tau)}{d\tau} = \frac{d\mathcal{C}_{u_i u_i}^T(\tau)/d\tau}{d\mathcal{C}_{u_i u_i}^S(\mathcal{S}_i(\tau))/d\mathcal{S}_i(\tau)} = u_d^T(\tau) = u' \sqrt{\mathcal{C}_{u_i u_i}^T(\tau)}, \quad (2.4)$$

where the last two equalities follow on differentiating (2.2) and from (2.3) respectively. Equation (2.4) provides another way to test the model when both the spatial and temporal correlations are known.

2.2. Temporal from spatial

We need to obtain the temporal correlation given the spatial correlation.

$$\mathcal{C}_{u_i u_i}^T(\tau(r_i)) = \mathcal{C}_{u_i u_i}^S(r_i) \quad (2.5)$$

with $\tau(r_i)$ being the *correlated time*, analogous to $\mathcal{S}_i(\tau)$ in equation (2.2):

$$\tau(r_i) = \int_0^{r_i} \frac{dr'_i}{u'_d}. \quad (2.6)$$

Further implementation requires the modelling of the velocity u'_d . When we consider two-point spatial velocity correlations, we have two sets of directions available, corresponding to the coordinates and the velocities respectively and thus we have both transverse and longitudinal velocity correlations. As discussed earlier, only the longitudinal velocity correlation is responsible for eddy decorrelation and hence only that should be considered in constructing the sampled RMS velocity field. We propose the following model to calculate u'_d :

$$(u'_d(r_z))^2 = w'^2 \mathcal{C}_{ww}^S(r_z) \quad (2.7)$$

with the scaling velocity, $u_s = w'$.

The time $\tau(r_z)$ brings in the temporal dependence associated with lengthscale r_z in the stationary spatial correlation: $\tau(r_z)$ and the associated decorrelation give the temporal correlation $\mathcal{C}_{ww}^T(\tau)$. Equations (2.5), (2.6) and (2.7) constitute the model for the longitudinal velocity correlations, schematically shown in figure 2(b).

To extend the model to the transverse correlation $\mathcal{C}_{ww}^S(r_x)$, we take the sampled velocity field in space to be

$$(u'_d(r_x))^2 = w'^2 \mathcal{C}_{ww}^S(r_x) \quad (2.8)$$

with the scaling velocity, $u_s = w'$, analogous to the longitudinal case (equation (2.7)).

Equations (2.5), (2.6) and (2.8) constitute the model for the transverse velocity correlations.

In this section we have used r_z and w' to denote the longitudinal direction and the velocity scale of isotropic turbulence. This is in anticipation of the application of the model to non-isotropic turbulence discussed next.

3. Results

We test the model using two-dimensional PIV measurements of pure buoyancy-driven turbulence in a vertical pipe (Cholehari 2004). The flow is driven by density difference $\Delta\rho$ across the ends of a circular pipe of length L and diameter d . The density difference is created using brine and water. There is no mean flow. The turbulence is axisymmetric. An axially homogeneous region exists in the middle of the pipe. The turbulence is not homogeneous in the lateral direction.

Typically, the density difference varies from 10 kg m^{-3} to about 2 kg m^{-3} . The dimensions of the pipe are $d = 50 \text{ mm}$ and $L = 45 \text{ cm}$. The Rayleigh number $g(\Delta\rho/\rho L)d^4/\nu\alpha$ is of the order of 10^8 . The Reynolds number based on Taylor microscale is about 100. The measurements are made in the middle of the pipe, in the axially homogeneous

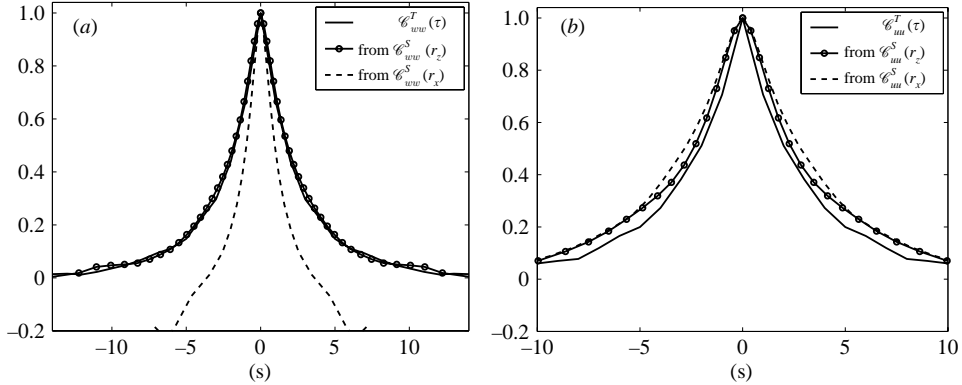


FIGURE 3. Temporal correlation from spatial correlations of velocity: (a) $\mathcal{C}_{ww}^T(\tau)$ from \mathcal{C}_{ww}^S ; (b) $\mathcal{C}_{uu}^T(\tau)$ from \mathcal{C}_{uu}^S ; z is the homogeneous direction. The solid lines are the measured temporal correlations.

region, in a plane passing through the pipe axis. The data consisting 270 velocity ‘frames’ span about ten minutes of the experiment.

Figure 3 gives the temporal correlations calculated from the spatial correlations of axial and lateral velocities, in the axial (z) and lateral (x) directions. Equations (2.5)–(2.8) are used. As described in §2.2, two choices exist for the spatial correlation in each case; the results of both choices are shown in the figure. In figure 3(a) the measured temporal correlation of the axial velocity, $\mathcal{C}_{ww}^T(\tau)$ is plotted along with the model predictions considering the spatial correlations in the axial ($\mathcal{C}_{ww}^S(r_z)$) and in the lateral directions ($\mathcal{C}_{ww}^S(r_x)$). The agreement with the model results is very good when $\mathcal{C}_{ww}^S(r_z)$ is used and poor when $\mathcal{C}_{ww}^S(r_x)$ is used. The former is a longitudinal correlation in the homogeneous axial direction, whereas the latter is a transverse correlation in the non-homogeneous direction. When the lateral velocity correlations $\mathcal{C}_{uu}^T(\tau)$ are considered (figure 3b), it is seen that the predictions from both the lateral ($\mathcal{C}_{uu}^S(r_x)$) and the axial ($\mathcal{C}_{uu}^S(r_z)$) directions are of about the same quality. In the experiments, the spatial correlation of the lateral velocity is nearly isotropic (spatial correlation maps were nearly circular). The choice of the direction of the correlation thus becomes less important. The model results are best when the longitudinal correlations in the homogeneous axial direction are considered, as expected.

Figures 4(a) and 4(b) give the model results for the case when the spatial correlation is predicted from the temporal correlation. Equations (2.1) to (2.3) are used in the calculation. As explained in §2.1, only the longitudinal correlation can be predicted in this case. Figure 4(a) gives the results of the predictions for the axial velocity correlations. The predictions are good. In the case of the lateral velocity correlations (figure 4b), the predictions are quite poor. Again, the model works best in the axial direction.

Figures 5(a) and 5(b) give the results of the model predictions for the cases where the transverse velocity correlations $\mathcal{C}_{ww}^S(r_x)$ and $\mathcal{C}_{uu}^S(r_z)$ are used to predict the temporal correlation. The scaling velocity according to the model corresponds to the velocity considered for the correlation, w' and u' respectively in the two cases. The effect of the alternative choice based on the direction, i.e. u' and w' respectively, is also shown in the figures. In figure 5(a), with the correlation function in the non-homogeneous direction, $\mathcal{C}_{ww}^S(r_x)$, the model prediction shows poor agreement with the measured temporal correlation. The alternative choice of the scaling velocity u' does slightly

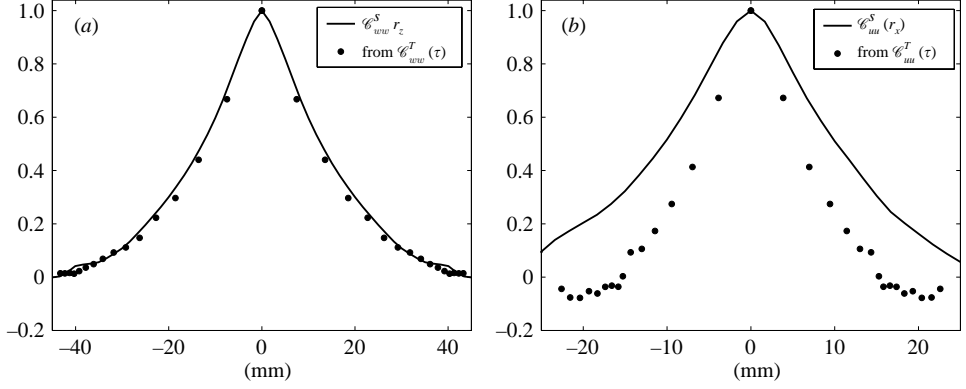


FIGURE 4. Spatial correlation from temporal correlation. (a) $\mathcal{C}_{ww}^S(r_z)$ from $\mathcal{C}_{ww}^T(\tau)$; (b) $\mathcal{C}_{uu}^S(r_x)$ from $\mathcal{C}_{uu}^T(\tau)$. Only the longitudinal correlation can be calculated. The solid lines are the measured spatial correlations.

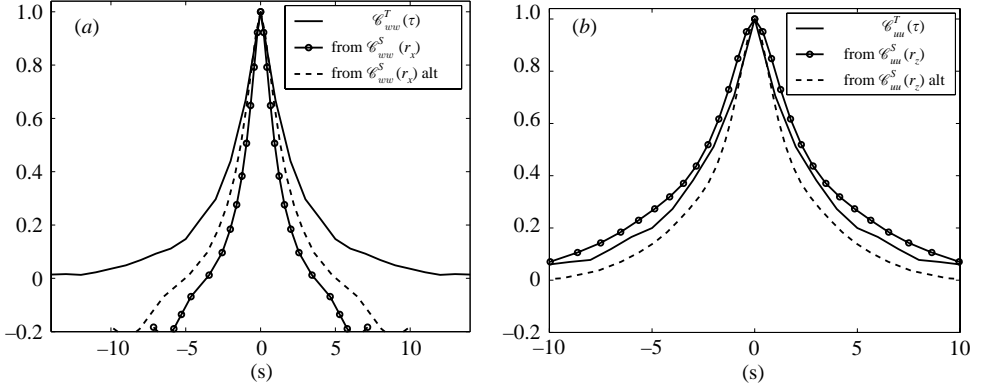


FIGURE 5. Temporal correlation from transverse spatial correlations. The solid lines are the measured temporal correlations. (a) Measured $\mathcal{C}_{ww}^T(\tau)$ compared with the model $u_s = w'$ (labelled $\mathcal{C}_{ww}^S(r_x)$) and with $u_s = u'$ (labelled $\mathcal{C}_{ww}^S(r_x)$, alt). (b) Measured $\mathcal{C}_{uu}^T(\tau)$ compared with the model $u_s = u'$ (labelled $\mathcal{C}_{uu}^S(r_z)$) and with $u_s = w'$ (labelled $\mathcal{C}_{uu}^S(r_z)$, alt).

better, but this may not be significant as the model itself is not really applicable in the non-homogeneous transverse direction. In figure 5(b), with the correlation function in the homogeneous direction, $\mathcal{C}_{uu}^S(r_z)$, the choice in the model, u' is slightly better compared to the alternative choice of w' . The difference is slight as the maps of constant \mathcal{C}_{uu}^S are nearly circular.

Another option is to handle the displacement through the longitudinal correlation, for example, in the case of $\mathcal{C}_{ww}^S(r_x)$ use $u' \sqrt{\mathcal{C}_{uu}^S(r_x)}$ to calculate the correlated time, i.e. treat the cross-correlation as one would handle the correlation of a passive scalar. But as mentioned earlier, we cannot link all the aspects of the information contained in the correlation consistently. This approach gave results which lie in between the two cases presented in figure 5(a), for example.

Figure 6 gives the results for the case when alternative models for the sampled velocities u_d^S and u_d^T are considered. Figure 6(a) is for the prediction of the temporal

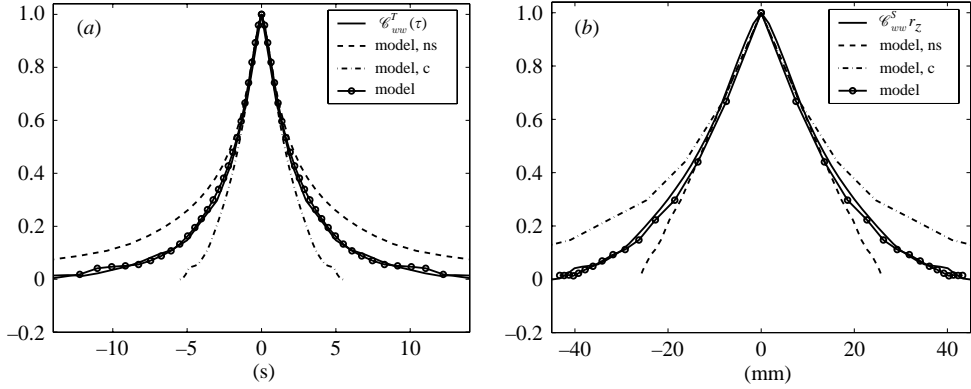


FIGURE 6. Alternative choices for the model. The model ($u_d^2 = w'^2 \mathcal{C}_{ww}^S$ and $w'^2 \mathcal{C}_{ww}^T$, respectively) is compared with $u_d = w'$ (model, c), and $u_d^2 = w'^2 (\mathcal{C}_{ww}^S)^2$ and $w'^2 (\mathcal{C}_{ww}^T)^2$, respectively (model, ns). (a) Temporal ($\mathcal{C}_{ww}^T(\tau)$) from spatial ($\mathcal{C}_{ww}^S(r_z)$) and (b) spatial ($\mathcal{C}_{ww}^S(r_z)$) from temporal ($\mathcal{C}_{ww}^T(\tau)$). The solid lines are the measured correlations.

correlation from the spatial correlation, and figure 6(b) is for the spatial from temporal case. Only the longitudinal velocity correlation in the homogeneous axial direction, $\mathcal{C}_{ww}^S(r_z)$, is considered for the comparison. The model is given by equation (2.8) in figure 6(a) and by (2.3) in figure 6(b). The alternative models considered were, firstly, when no attenuation is present in the dispersion velocity, $u_d^S = w'$ or $u_d^T = w'$, and secondly, when the dispersion is attenuated by the square of the correlation function, $(u_d^S)^2 = w'^2 (\mathcal{C}_{ww}^S(r_z))^2$ or $(u_d^T)^2 = w'^2 (\mathcal{C}_{ww}^T(\tau))^2$. In both figures, it is seen that the standard model does best overall, over the entire extent of the correlation. However, there is not much difference amongst the three at small times (or for small separation distances), where the correlations are close to unity and all three models are nearly equivalent. As expected, the constant model, with its lack of attenuation, underpredicts the correlation in the temporal-from-spatial case (the correlated time is less than the actual time) and overpredicts the correlation in the spatial-from-temporal case (the correlated displacement is more than the actual displacement). For the second choice of the model, where the attenuation $(\mathcal{C}_{ww}^S(r_z))^2$ or $(\mathcal{C}_{ww}^T(\tau))^2$ is more than the model (as the correlations are less than unity), the behaviour is opposite – the model overpredicts the temporal-from-spatial case and underpredicts the spatial-from-temporal case. The choice of the model, (2.3) or (2.8), based on physical arguments involving eddy correlation, seems to work best.

4. Discussion

The model results are encouraging, especially with the longitudinal correlations in the homogeneous axial direction along the axis of symmetry (figures 3a, 4a). The model does poorly with the transverse correlations (figure 5). The model does not do well along the non-homogeneous directions (figures 3b, 4b).

The small eddies are embedded in the larger eddies and are swept by them. The velocities used to calculate the spatial or temporal correlation functions are obtained at fixed points, and would be subject to sweeping by the large eddies. Thus the velocities obtained in the model (equations (2.3) and (2.7)) also include the sweeping effects, and thus the sweeping effect is incorporated in the model.

To apply the model with a mean flow, we need to assume local axisymmetry of the fluctuations along the mean flow direction (which is a reasonable assumption, as shown in George & Hussein 1991). The eddy decorrelation occurs because of both the mean convection and the turbulence evolution. Thus we need to augment the mean convection velocity with the sampled RMS velocity (2.3) when calculating the spatial separations from temporal separations.

The validity of the model can be tested using results from DNS studies.

REFERENCES

- ANTONIA, R. A., PHAN-THIEN, N. & CHAMBERS, A. J. 1980 Taylor's hypothesis and the probability density functions of temporal velocity and temperature derivatives in a turbulent flow. *J. Fluid Mech.* **100**, 193–208.
- BROUWERS, J. J. H. 2004 Eulerian short-time statistics of turbulent flow at large Reynolds number. *Phys. Fluids* **16**, 2300–2308.
- BROWNE, L. W. B., ANTONIA, R. A. & RAJAGOPALAN, S. 1983 Spatial derivative of temperature in a turbulent flow and Taylor's hypothesis. *Phys. Fluids* **26**, 1222–1233.
- CHOLEHARI, M. R. 2004 Buoyancy driven turbulence in a vertical pipe. PhD thesis, Department of mechanical engineering, Indian Institute of Science.
- CHEN, S. & KRAICHNAN, R. H. 1989 Sweeping decorrelation in isotropic turbulence. *Phys. Fluids A* **1**, 2019–2024.
- DAHM, W. J. A. & SOUTHERLAND, K. B. 1997 Experimental assessment of Taylor's hypothesis and its applicability to dissipation estimates in turbulent flows. *Phys. Fluids* **9**, 2101–2107.
- FAVRE, A. J. 1965 Review on space-time correlations in turbulent fluids. *Trans. ASME, J. Appl. Mech.* **32**, 241–257.
- FAVRE, A. J., GAVIGLIO, J. J. & DUMAS, R. 1957 Space-time correlations and turbulent spectra in a turbulent boundary layer. *J. Fluid Mech.* **2**, 313–342.
- FAVRE, A. J., GAVIGLIO, J. J. & DUMAS, R. 1958 Further on space-time correlations and turbulent spectra in a turbulent boundary layer. *J. Fluid Mech.* **3**, 344–356.
- FISHER, M. J. & DAVIES, P. O. A. L. 1964 Correlation measurements in a non-frozen pattern of turbulence. *J. Fluid Mech.* **18**, 97–116.
- HESKESTAD, G. 1965 A generalized Taylor hypothesis with application for high Reynolds number turbulent shear flows. *J. Appl. Mech.* **87**, 735–739.
- GEORGE, W. K. & HUSSEIN, H. J. 1991 Locally axisymmetric turbulence. *J. Fluid Mech.* **233**, 1–23.
- GLEDZER, E. 1997 On Taylor hypothesis corrections for measured energy spectra of turbulence. *Physica D* **104**, 163–183.
- LEBOEUF, R. L. & MEHTA, R. D. 1995 On using Taylor's hypothesis for three-dimensional mixing layers. *Phys. Fluids* **7**, 1516–1518.
- LIN, C. C. 1953 On Taylor's hypothesis and the acceleration terms in the Navier-Stokes equations. *Q. Appl. Maths* **10**, 295–306.
- LUMLEY, J. L. 1965 Interpretation of time spectra measured in high intensity shear flows. *Phys. Fluids* **8**, 1056–1062.
- NELKIN, M. & TABOR, M. 1990 Time correlations and random sweeping in isotropic turbulence. *Phys. Fluids A* **2**, 81–83.
- PINSKY, M., KHAIN, A. & TSINOBER, A. 2000 Accelerations in isotropic and homogeneous turbulence and Taylor's hypothesis. *Phys. Fluids* **12**, 3195–3204.
- PIOMELLI, U., BALINT, J.-L. & WALLACE, M. 1989 On the validity of Taylor's hypothesis for wall-bounded flows. *Phys. Fluids A* **1**, 609–611.
- RILEY, J. J. & PATTERSON JR., G. S. 1974 Diffusion experiments with numerically integrated isotropic turbulence. *Phys. Fluids* **17**, 292–297.
- SQUIRES, K. D. & EATON, J. K. 1989 Lagrangian and Eulerian statistics obtained from direct numerical simulations of homogeneous turbulence. *Phys. Fluids A* **3**, 130–143.
- TAYLOR, G. I. 1938 The spectrum of turbulence. *Proc. R. Soc. Lond A* **132**, 476–490.
- TENNEKES, H. 1975 Eulerian and Lagrangian time microscales in isotropic turbulence. *J. Fluid Mech.* **67**, 561–567.

- TSINOBER, A., VEDULA, P. & YEUNG, P. K. 2001 Random Taylor hypothesis and the behaviour of local and convective accelerations in isotropic turbulence. *Phys. Fluids* **13**, 1974–1984.
- WYNGAARD, J. C. & CLIFFORD, S. F. 1977 Taylor's hypothesis and high frequency turbulence spectra. *J. Atmos. Sci* **34**, 922–929.
- YEUNG, P. K. 2001 Lagrangian statistics of turbulence and scalar transport in direct numerical simulations of turbulence. *J. Fluid Mech.* **427**, 241–274.
- YEUNG, P. K. 2002 Lagrangian investigations of turbulence. *Annu. Rev. Fluid Mech.* **34**, 115–142.
- YEUNG, P. K. & POPE, S. B. 1989 Lagrangian statistics from direct numerical simulations of isotropic turbulence. *J. Fluid Mech.* **207**, 531–586.
- YEUNG, P. K. & SAWFORD, B. L. 2002 Random-sweeping hypothesis for passive scalars in isotropic turbulence. *J. Fluid Mech.* **459**, 129–138.
- ZAMAN, K. B. M. Q. & HUSSAIN, A. K. M. F. 1989 Taylor hypothesis and large-scale coherent structures. *J. Fluid Mech.* **112**, 379–396.